Optimization of Solar Still Performance using Computational Fluid Dynamics and Taguchi Method

[1]Vivek Kumar Tripathi, [2]Dr. Shashi Kant Sharma
Department of Mechanical Engineering, People's University Bhopal
Department of Mechanical Engineering, People's University Bhopal
Email-: [1]vtripathi2801@gmail.com [2]shashikant_sharma@peoplesuniversity.edu.in

* Corresponding Author: Vivek Kumar Tripathi

Abstract: *Solar stills offer a sustainable solution for producing potable water by utilizing solar energy. This paper explores the optimization of solar still performance through computational fluid dynamics (CFD) analysis and the Taguchi method. A comprehensive review of solar still operation and design is provided, highlighting the need for increased water productivity and cost efficiency. The study focuses on a single-slope solar still design, considering factors such as glass thickness and slope angle to enhance water production. The Taguchi method is applied to identify optimal parameter settings, and CFD simulations are conducted to evaluate the performance of the solar still under varying conditions. Results show that increasing slope angle can initially improve water vapor density but may lead to reduced condensation efficiency at higher angles. Through optimization, significant improvements in mass flow rate and productivity are achieved, validating the effectiveness of the proposed approach.*

Keywords: *Solar still, Computational fluid dynamics, Taguchi method, Optimization, Water productivity, Sustainability*.

I. INTRODUCTION

A solar still distills water, using the heat of the Sun to evaporate, cool then collect the water. There are many types of solar still, including large scale concentrated solar stills, and condensation traps (better known as moisture traps amongst survivalists). In a solar still, impure water is contained outside the collector, where it is evaporated by sunlight shining through clear plastic or glass [1–3]. The pure water vapor condenses on the cool inside surface and drips down, where it is collected and removed [4].

Distillation replicates the way nature makes rain. The sun's energy heats water to the point of evaporation. As the water evaporates, water vapor rises, condensing into water again as it cools and can then be collected. This process leaves behind impurities, such as salts and heavy metals, and eliminates microbiological organisms. The end result is pure distilled water [5–8].

A solar still consist of shallow triangular basin made up of Fiber Reinforced Plastic (FRP). Bottom of the basin is painted black so as to absorb solar heat effectively. Top of the basin is covered with transparent glass tilt fitted so that maximum solar radiation can be transmitted in to the still. Ages of the glass are sealed with the basin using tar tape so that the entire basin becomes air tight. Entire assembly is placed on a structure made of MS angle. Out let is connected with a storage container. Provision has been made to fill water in the still basin. A window is provided in the basin to clean the basin from inside. Water is charged in to the basin in a thin layer.

The available fresh water on earth is limited. More than two-third of the earth's surface is covered with water but more than 97% of the available water is either salty or polluted. Rest nearly around 2.6% is fresh water. Less than 1% of fresh water is within reach of human and other organism. Even this small fraction is believed to be adequate to support life on earth but fresh water demand is increasing day by day due to increasing population (Tiwari et al., 2003; Kumar et al., 2015). Polluted water cannot be used directly for drinking purpose as it has harmful microbes and dissolved substance. Many developed and developing countries of the world are facing the problem of supply of drinking water and fresh water. The methods for production of fresh water used now a day are as follows: reverses osmosis, multi effect distillation, and mechanical vapor compression, etc. These methods involve major drawback of energy consumption in purification. Solar thermal desalination method is best suited for the fresh drinking water production at low cost. Interest in solar distillation systems is more because of their easy to operate and very less maintenance cost.

A. Diffusion still

In this type of still, two surfaces which are maintained at hot and cold temperatures are held parallel to each other. The schematic of diffusion still. The gap thickness between these surfaces is kept very small to suppress convective heat transfer. The hot surface acts as a membrane between the cold side and the glass cover. Thermal energy from the sun is absorbed by the front side of this membrane. As water flows through the membrane, it evaporates and diffuses through the gap and gets condensed on the cold side. This water then gets collected into a container due to gravity. There have been many design modifications in the solar still since its conception. These modifications incorporated regulation of parameters affecting the solar still performance, the coupling of two or more distillation processes or the addition of a separate mechanism to enhance the productivity of the stills.

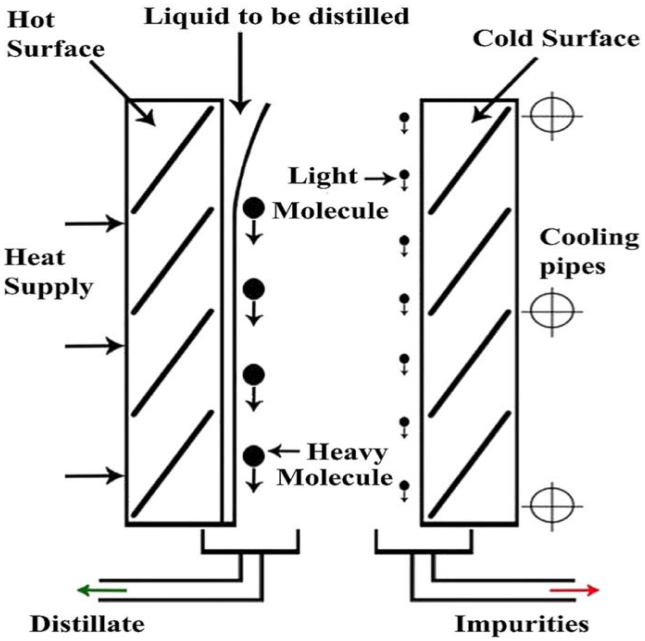

Fig. 1 Diffusion still

B. Drawbacks of solar stills

The main drawbacks of solar stills involve the requirement of large installation areas, lower productivity and higher land cost associated with the larger land requirement (Ayoub and Malaeb 2012). So, the studies mainly focus on enhancing the water production from solar still to negate the limitations as well as on keeping the unit cost of water as low as possible. According to Abujazar et al. (2016), the productivity of a solar still is influenced by ambient conditions (solar radiation, ambient temperature, wind velocity, etc.), operating conditions (brine water depth, saline concentration, etc.) and design conditions (cover angle, insulation, etc.). The behavior of solar stills with different configurations and different working conditions has been widely studied over the past few decades. Since the distribution of solar radiation around the world is non-uniform, the performance studies of solar still are required to be replicated under the climatic condition of Bhopal. the condition of Bhopal is in favor of the solar still application for drinking water production. In addition, solar still is easy to construct with local labor force using low-cost readily available materials and even illiterate people can operate solar still due to its very simple operations, which make it an excellent choice in the context of Bhopal.

II. LITERATURE REVIEW

Da Silva Junior et al. (2023): colleagues address the pressing need for potable water by exploring the efficiency of a low-cost solar still through numerical modeling. Their study, conducted under Brazilian climatic conditions, predicts the device's performance without experimental measurements. Results indicate that smaller water volumes and higher global radiation intensity lead to increased efficiency, with optimal water production observed after 30 minutes.

Aghakhani et al. (2023):. propose innovative enhancements to traditional solar stills, integrating basin water heating, glass cooling, and operational pressure reduction to optimize water production. Utilizing numerical simulations and machine learning algorithms, they demonstrate significant performance improvements, highlighting the potential for enhanced potable water production.

Hammoodi et al. (2023): provide a comprehensive overview of parameters affecting pyramid solar still performance, emphasizing the significant influence of meteorological, design, and operating factors. Their review underscores the potential for increased productivity through design modifications, including the use of phase change materials and reflectors.

Arunkumar et al. (2022): solar distillation of real wastewaters and seawater, demonstrating effective pollutant removal through solar evaporation. Their analysis highlights the viability of solar stills in wastewater treatment, with notable pollutant reduction rates observed across various wastewater types.

Shoeibi et al. (2022):. evaluate the use of hybrid nanofluid glass cooling in double-slope solar stills, demonstrating significant improvements in freshwater yield and energy efficiency. Their findings suggest that hybrid nanofluid cooling enhances heat transfer within the solar still, contributing to enhanced water production.

Sonawane et al. (2022): conduct a parametric analysis of solar still desalination systems, investigating the impact of different absorber materials on system performance. Through computational fluid dynamics simulations, they identify black toner as a promising absorber material, offering improved productivity and environmental benefits.

S. El-Sebaey et al. (2020): develop a computational fluid dynamics model to predict the performance of basin-type solar stills without experimental measurements. Their simulation results, validated under specific climatic conditions, demonstrate good agreement with experimental data, highlighting the potential of CFD modeling in solar still optimization.

Nadgire et al. (2020): design and analyze a double-effect passive solar still for freshwater production, employing experimental investigations and numerical simulations. Their findings suggest good agreement between experimental and simulation results, showcasing the potential of solar stills in addressing freshwater scarcity.

Shanmugan et al. (2020): investigate the performance of solar stills under different operating conditions, including the use of TiO2 nanoparticles and hybrid bond adsorption. Their study demonstrates enhanced water production, particularly during winter and summer conditions emphasizing the importance of design optimization.

III. OBJECTIVES

- To increase the productivity of solar still by varying geometrical parameters
- To optimize the mass flow of solar still
- Compare the conventional results by new proposed design of solar still
- To analyze the temperature, mass flow and to optimize the efficiency of solar still
- By compare all parameter solar still to validate the analytical from the conventional design

IV. RESEARCH METHODOLOGY

A solar still is a simple device that utilizes solar energy to produce fresh water. Single slope solar still. It is composed of a glass housing that allows smaller wave length radiations (A) to enter the solar still but does not allow larger wavelength radiations to escape the glass housing, thus producing a high temperature within the solar due to the greenhouse effect. The roof of solar still, is made of glass, is tilted at a specific slope to allow the maximum possible direct solar radiations to enter the solar still. As the solar radiations fall on the glass roof of the solar still a small fraction of it is reflected out by the glass (β), a part of it is absorbed by the glass (C), while the remaining part enters the solar still. The sides of the solar still are made up of glass as well. The glass sides allow the shorter wavelengths coming from direct radiations to enter the solar still. However, longer wavelength radiations are not able to escape the solar still due to the greenhouse effect.

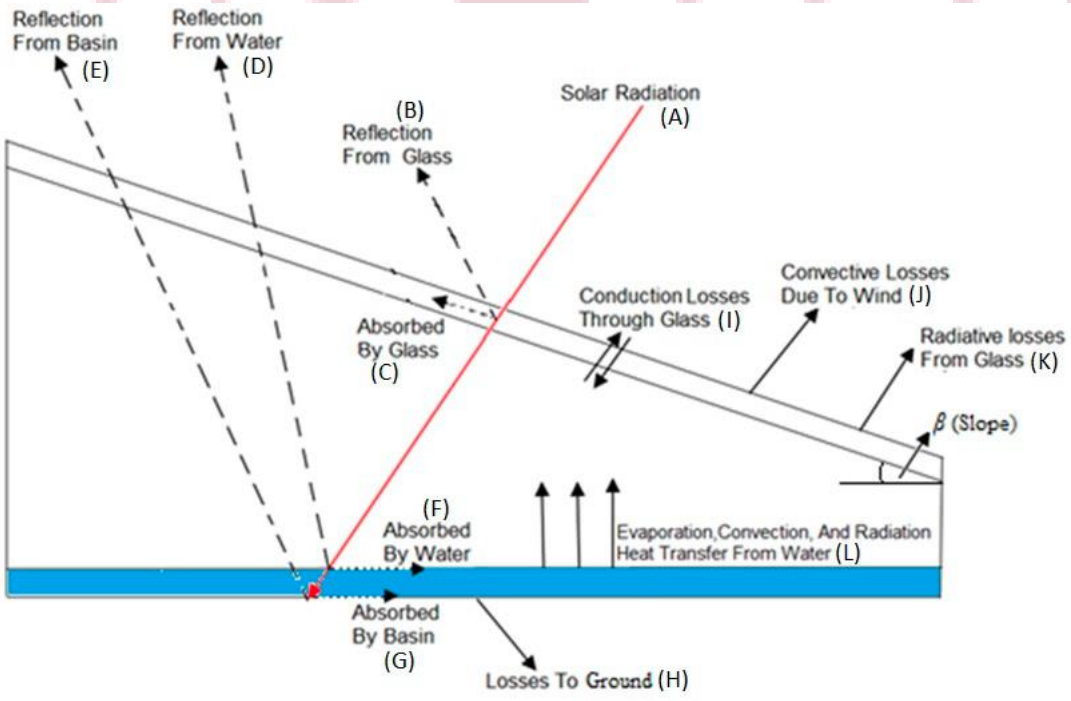

Fig. 2 Single slope solar still

If brackish water (saline water) is placed inside the basin of the solar still, a part of the solar energy will also be reflected by the brackish water (D) as well as the basin material (E). There will also be some losses of energy to the ground (H),

whereas the remaining solar energy that has entered the solar still will be absorbed by the brackish water (F) and the basin (G). This absorbed solar energy by the brackish water causes evaporation inside the solar still (L). The evaporated water is pure (without any contamination) and is drawn out by convection to come into contact with the inner surface of the glass roof. Thus, the inner surface of the glass housing, being in contact with the evaporated water, is at a comparatively higher temperature. The outer surface of the glass housing is at a comparatively lower temperature, being in contact with outside air. Hence, the temperature gradient between the inner and outer surfaces of the glass housing allows conduction heat transfer (I), resulting in the condensation of pure water, which is then collected as fresh water. During the process, a small fraction of energy is lost by the convective losses (J) due to the wind and the radiative losses from the glass (K). The left-over brackish water inside the basin of the solar still becomes more concentrated and is later removed and replaced with new brackish water.

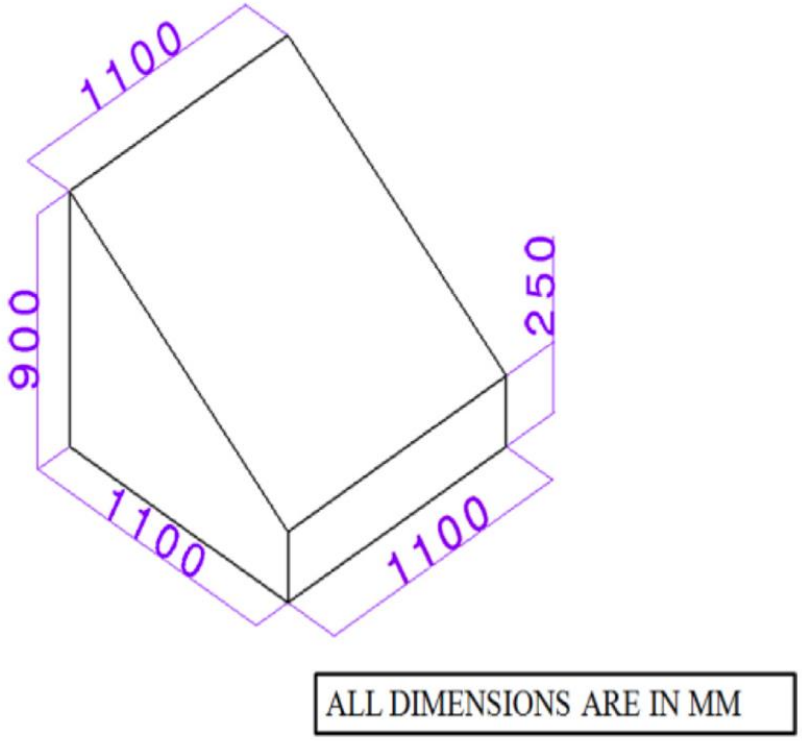

Fig. 3 Geometry of single slope solar still (Gnanavel et al. 2020)

A. Assumptions

Predicting the output and performance of a solar still requires mathematical modeling validated by simulation results. Mathematically, solar still performance is evaluated by the thermal analysis of the system. The thermal analysis includes heat transfer calculations performing energy balance, resulting in evaluating the efficiency of the system. However, the performance of such systems is strongly dependent on solar radiation data and the ambient conditions which behave as input parameters within this mathematical model. The following assumptions are made while developing the code to evaluate the energetic performance of the solar still:
(i) Steady-state conditions occur during the time interval (steady operation over an hour).
(ii) No vapor can escape from the still (no vapor leakage).
(iii) The heat capacity of the glass cover, thermoelectric module surface and basin liner is negligible.
(iv) The level of saline water remains constant in the basin.

B. Productivity and thermal efficiency

In the current work, the productivity of potable water was collected at each experimental hour. The daily or total productivity, which is the amount of the cumulated fresh water within the daily working hours (d.w.h) of the solar still, is calculated from:

$$P_d = \sum_1^{d.w.h} P_h$$

The fresh water productivity enhancement ($p_{enh.}$) of solar still is evaluated as:

$$P_{enh.} = \frac{(P_d)m - (P_d)c}{(P_d)c} x100\%$$

(pd)m and(pd)c are the total productivity of freshwater from the modified and conventional solar still, respectively.

The hourly thermal efficiency of solar still is defined as the ratio of the heat transfer per unit mass (qe) by evaporation–condensation in the still to the incident solar radiation (I) in the still.

$$\eta = \frac{q_e}{I} x100 = \frac{h_{ewg}(T_w - T_{gi})}{I}\ x\ 100\%$$

The hourly productivity of fresh water in (kg/h) is defined as follows:

$$Ph = \frac{h_{ewg} A_b (T_w - T_{gi})}{L}\ x\ 3600$$

So, the hourly thermal efficiency of solar still is calculated as follows:

$$\eta = \frac{P_h x\ L}{A_g x\ I\ x\ 3600} x\ 100\%$$

Thus, the total thermal efficiency of solar still is expressed as follows:

$$\eta_t = \frac{P_d X L_{av}}{A_g X \sum_1^{d.w.h} I\ X\ 3600}\ X\ 100\%$$

L is calculated based on ref. [36] in J/kg as follows or using online tables [37]

$$L = (2503.3\text{-}2.398\ X\ Tw\ X\ 10^3$$

C. Parameters and Levels

The Taguchi method, developed by Genichi Taguchi, is a statistical approach to optimization that is widely used in engineering and quality control. It helps in optimizing performance and minimizing variation in manufacturing processes. When applying the Taguchi method to select parameters, such as in experimental design, the following steps are generally involved:

- Identify the Factors (Parameters): Clearly define the factors (independent variables or parameters) that may influence the performance of the system or process.
- Determine the Levels of Each Factor: Specify the different levels or settings for each factor that will be tested. These levels should cover the potential range of variation for each factor.
- Define the Experimental Design: Use the orthogonal array provided by Taguchi to plan the experiments efficiently. The orthogonal array helps to reduce the number of experimental runs while still capturing the main effects and interactions.
- Select the Performance Measure (Response): Clearly define the performance measure or response variable that you want to optimize. This could be a measure of quality, efficiency, or any other relevant metric.
- Conduct Experiments: Perform the experiments based on the designed orthogonal array. Each combination of factor levels represents a unique experimental run.
- Collect Data: Record the data for each experimental run, including the performance measure or response variable.
- Analyze Data: Use statistical methods to analyze the collected data. Taguchi uses signal-to-noise (S/N) ratios to evaluate the effect of each factor and the interaction between factors.
- Identify the Optimal Parameter Settings: Determine the combination of factor levels that provides the optimal performance or the highest S/N ratio.
- Conduct Confirmation Runs: Validate the results by conducting confirmation runs with the identified optimal parameter settings.

Based on the previous studies, glass thickness and slope have been selected as a input parameter (Ali et al., 2023). The range of slope angle has been varied from 20° to 30° with three levels and glass thickness was varied from 0.01 to 0.02 mm (see Table 4.1). These two parameters are input parameters which was varied to examine performance parameters such as mass flow rate. The three parameter with three levels constituents nine simulation based on L9 orthogonal array. Based on Table 3.2, total nine models and nine simulation was done by varying slope angle and solar intensity.

Table 1 Parameter and range

	I	II	III
Slope	20°	25°	30°
Glass thickness	0.01	0.02	0.03

Table 2 L9 orthogonal array

Run	Slope	Glass thickness, m
1	20º	0.01
2	25º	0.02
3	30º	0.03
4	20º	0.02
5	25º	0.03
6	30º	0.02
7	20º	0.03
8	25º	0.01
9	30º	0.02

D. Computational Fluid Dynamics Analysis of Solar Still

Computational fluid dynamics involves the analysis of fluid flow and heat transfer systems through computer-based simulations. This powerful technique finds applications across diverse industrial and non-industrial domains. The present study utilizes a phase-shifting substance for CFD assessments in solar stills, employing ANSYS Fluent for the simulations. The mathematical model includes expressions for conservation of momentum and energy.

The core of CFD lies in mathematical approaches addressing fluid flow challenges. Computational Fluid Dynamics software provides comprehensive user interfaces for inputting variables, examining details, and accessing solution capabilities promptly. Therefore, three main components are employed to address and solve Computational Fluid Dynamics problems.

1) Pre-processor,
2) Solver and
3) Post-processor.

Pre-processor

In order for a Computational Fluid Dynamics program to properly analyse flow issues, it is essential to go through pre-processing. This involves inputting the issue through a user-friendly interface and converting it into a format that the solver can interpret. During this phase, the customer is responsible for ensuring an accurate input:

- Define the shape of the area of interest: the computationally region.
- Grid production — the partition of a region into small units, such as a grid (or mesh) of units (or control volumes or components).
- Choosing which physical and chemical processes should be modelled.
- Fluid characteristics are defined.
- Determination of suitable boundary conditions.

At nodes within each cell, the solutions to a flow issue (velocity, pressure, temperature, etc.) are specified. The amounts of cells inside the grids determines the reliability of a CFD result. In general, the higher the quantity of cells, the more accurate the result. In the end, such systems will modify the grid automatically in places with quick fluctuations. Before all these approaches are robust sufficient to be included into commercial CFD programmes, a substantial portion of fundamental development work must be accomplished.

Solver

Mathematical solution approaches are divided into three categories: finite differences, finite elements, as well as spectral approaches. A particular finite differential framework, including such CFX/ANSYS, FLUENT, PHOENICS, and STAR-CD, is used in CFD issues.

The mathematical algorithm in this stage involves the following steps:

• Complete integration of governing fluid circulation equations across all control volumes within the domain.
• The discretization process involves transforming the resulting integral equations into an algebraic framework.
• Application of an iterative method to solve the mathematical equation.

The primary step in the finite volume approach, which sets it apart from other CFD methods, is the integration of the control volume. The resulting statements for each finite-sized cell outline the exact conservation of crucial attributes. The conservation of a general flow variable φ, such as a velocity component or enthalpy, within a finite control volume is articulated as an equilibrium between the diverse processes working to either increase or decrease it.

Post-processor

As we move forward with our analysis, we may also be interested in delving deeper into the outcomes. At this particular stage, our goal is to fully examine and evaluate the results:

- Domain geometry and grid display
- Line and shaded contour plots
- 2D and 3D surface plots
- Colour Post Script output

- Vector plots
- contour diagrams

These features may now incorporate animation for variable outcome presentation, and all codes offer dependable alpha-numeric outputs as well as data export capabilities for further processing.

Algorithm used for Computational fluid dynamics analysis:

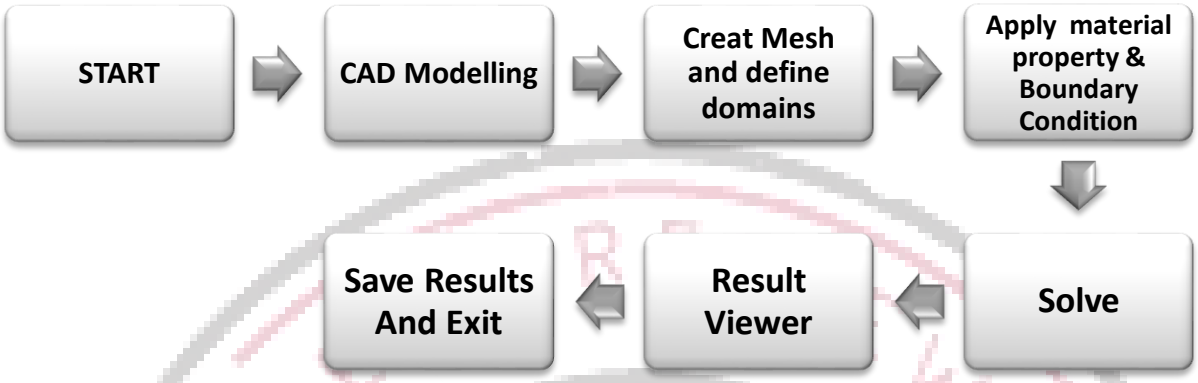

Fig. 4 Algorithm used for CFD analysis

E. Boundary conditions

- Set gravitational acceleration in –y direction as 9.81 m/s^2 for flowing of fluid due to natural convection.
- Use multi-phase model as VOF (Volume of fluid).
- Need to on energy equation, though heat transfer takes place.
- In Viscous model select k-epsilon with standard wall function turbulence model
- Solar radiations were used on glass cover of the solar still with global position of longitude 77.4^{o}E, latitude 23.2599^{o}N, time zone GMT+5:30 for the fair weather condition for Bhopal region.
- In the complex process of evaporation-condensation, multiple phases interact to facilitate the transfer of mass through both vapour-to-vapour and vapour-to-water mechanisms.
- In phase interaction, continuum surface force and wall adhesion with constant surface tension coefficients of 0.07 N/m.
- Opt for the Second Order Upwind scheme for solving the Momentum and Energy equations.
- The Fluent solver is employed to address the computational fluid dynamics (CFD) challenge.

The imposition of boundary conditions in the study involved a combination of deductions from physical phenomena and simulations carried out in the ANSYS CFD software. The categorization of boundary conditions for different sections of the solar still, along with their respective types, is presented. To facilitate their selection in the CFD simulation work, real or physical boundary conditions were normalized and idealized. As an illustration, the side walls of the solar still, treated as adequately insulated, were assumed to possess a heat flux of zero. Further details regarding the input parameters for the CFD analysis are outlined.

Table 3 Boundary Conditions

Boundary Name	Type	Thermal conditions	Body type
Absorber plate	Wall	Adiabatic wall (Heat flux = 0)	Opaque
Front wall	Wall	Adiabatic wall (Heat flux = 0)	Opaque
Back wall	Wall	Adiabatic wall (Heat flux = 0)	Opaque
Glass	Wall	Constant Heat flux (1000 W/m^2)	Semi-transparent
Side wall (left)	Wall	Adiabatic wall (Heat flux = 0)	Opaque
Side wall (right)	Wall	Adiabatic wall (Heat flux = 0)	Opaque

Table 4 CFD analysis Input parameters.

Setup		Descriptions
General	General	Absolute velocity formulation, pressure based steady state analysis. Gravity = -9.81 m/s^2 in y-direction
Model	Multiphase	Volume of fluid, Implicit formulation, Sharp Interface modelling Number of Eulerian phase = 3
	Energy	On
	Viscous	K-epsilon, Standard model with Standard wall function
	Radiation	Rosseland Radiation Model, Solar Ray Tracing method with Direct solar irradiation = 1000 W/m^2, Longitude 77.4ºE, Latitude 23.2599ºN, Time zone GMT+5:30 hour
Materials	Fluid	Air, Water-liquid, Water-vapour
	Solid	Glass, Steel, Wood
Phase	Primary	Air, Mass transfer mechanism : evaporation-condensation
	Secondary-1	Water-liquid, Mass transfer mechanism : evaporation-condensation
	Secondary-2	Water vapor, Mass transfer mechanism : evaporation-condensation
Solution	Pressure-Velocity coupling, Scheme- SIMPLE. Spatial Discretization: Momentum- Second order Upwind, Volume fraction- Compressive, Turbulent KE & Dissipation rate- Second order Upwind, Energy- Second order Upwind	

V. RESULT AND DISCRE

The main objective of the present work is to determine the maximum output of water that is able to be produced from the double slope solar still basin and compare their efficiency for the validation of the work on research paper of C. Gnanavel et al 2020, "CFD analysis of solar still with PCM", Materials Today: Proceedings, Available online at ScienceDirect, accepted 24 May 2020. doi.org/10.1016/j.matpr.2020.05.638. has been studied and perform computational fluid dynamics analysis by creating three-dimensional CAD model of single and double slope solar still using ANSYS design modular having the dimensions of base 1.1 m x 1.1 m, front wall dimensions of 0.25 m in height and back wall of 0.9 m for single slope. The obtain results have been compared with published literature.

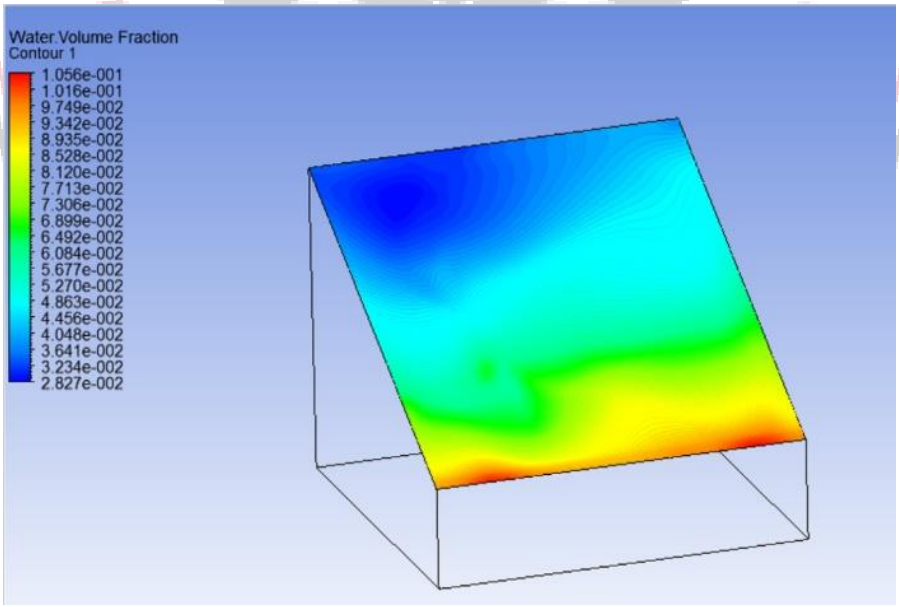

Fig. 4. Water Volume Fraction on Glass *[C. Gnanavel et al 2020]*

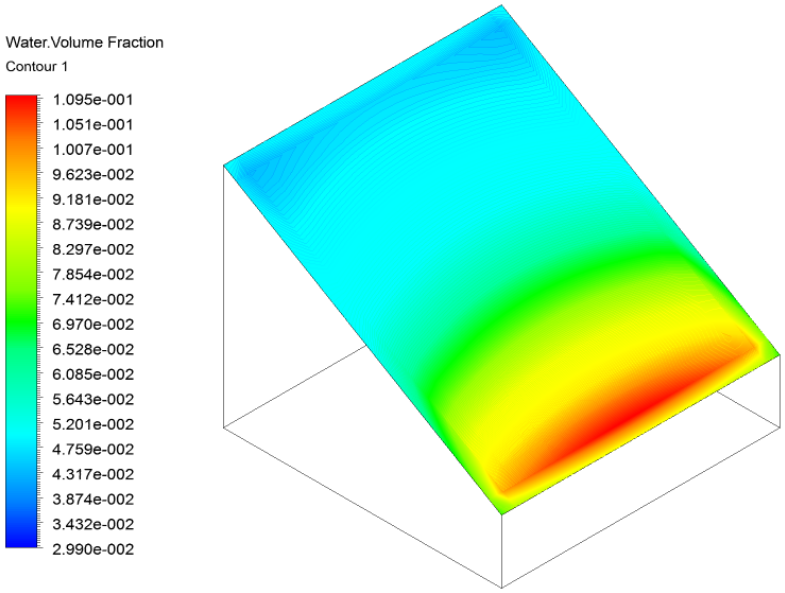

Fig. 5. Water Volume Fraction on Glass *[Present study]*

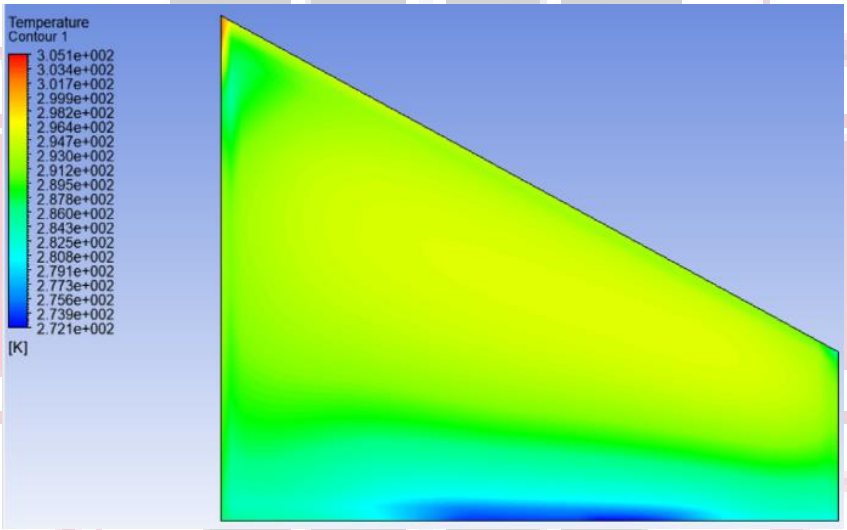

Fig. 6. Temperature on Glass *[C. Gnanavel et al 2020]*

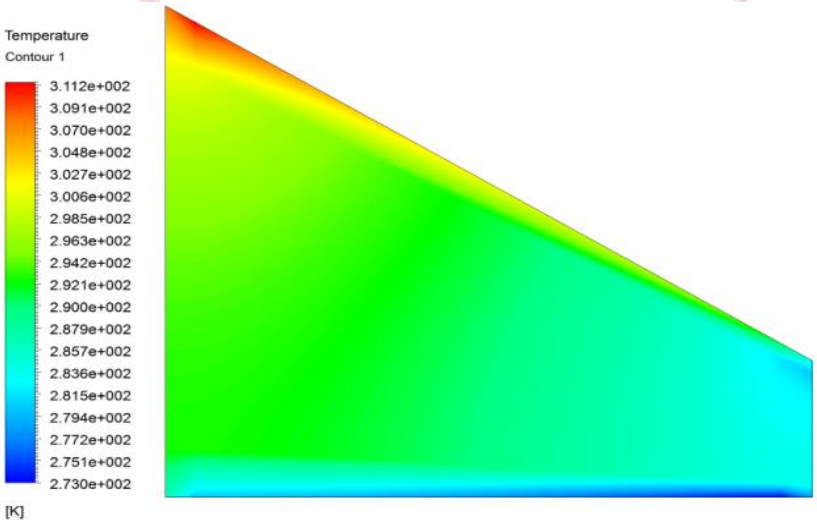

Fig. 7. Temperature on Glass *[Present study]*

From the above contour diagrams (fig. 4.1 to fig. 4.4) it has been observed that Volume fraction of water showing 3.69% variation while the temperature difference of 6.1 degree showing 1.99% variation. All above compared results show very good agreement between base paper and present work, hence the further analysis with same boundary with modified design have to be done.

Table 5 different parameter compared with C. Gnanavel et al 2020& present work:

S. No	Parameters	C. Gnanavel et al (2020)	Present work	% Difference
1	Water Volume Fraction on Glass	0.1056	0.1095	3.69%
2	Temperature (K)	305.1	311.2	1.99%

A. Computational fluid dynamics analysis of single slope solar still

After performing computational fluid dynamics analysis on single slope solar still for mass flow of condense liquid following contour has been observed on a section in X-Y plane and at Z = 0.55 m, the maximum value of mass flow rate of 2.198e-2 kg/s-m^2 as shown in figure 4.5.

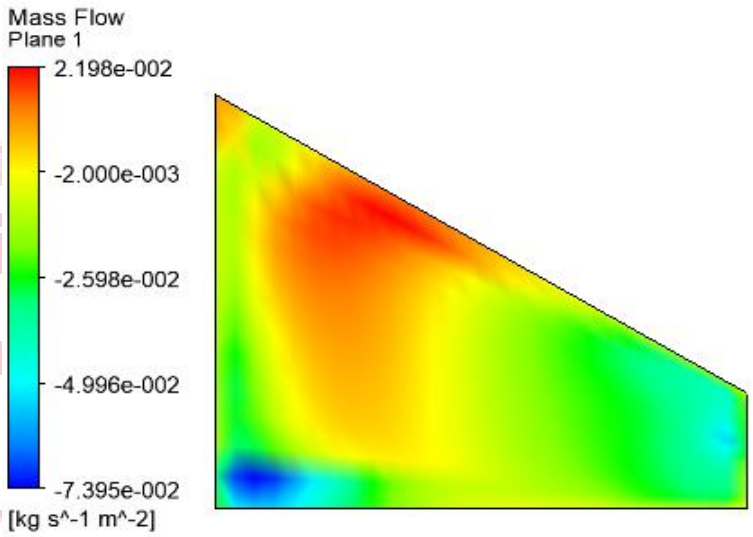

Fig. 8. Contour result of mass flow in the solar still for model 1

After performing computational fluid dynamics analysis on single slope solar still for mass flow of condense liquid following contour has been observed on a section in X-Y plane and at Z = 0.55 m, the maximum value of mass flow rate of 1.961e-2 kg/s-m^2 as shown in figure 4.6.

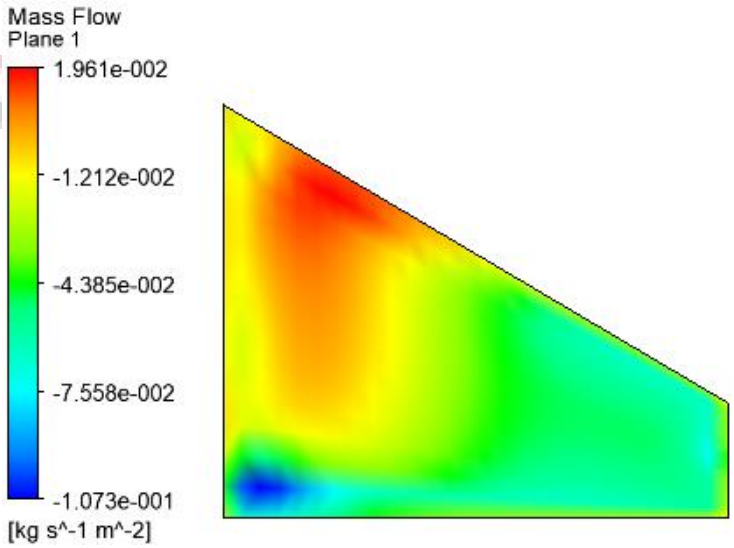

Fig. 9. Contour result of mass flow in the solar still for model 2

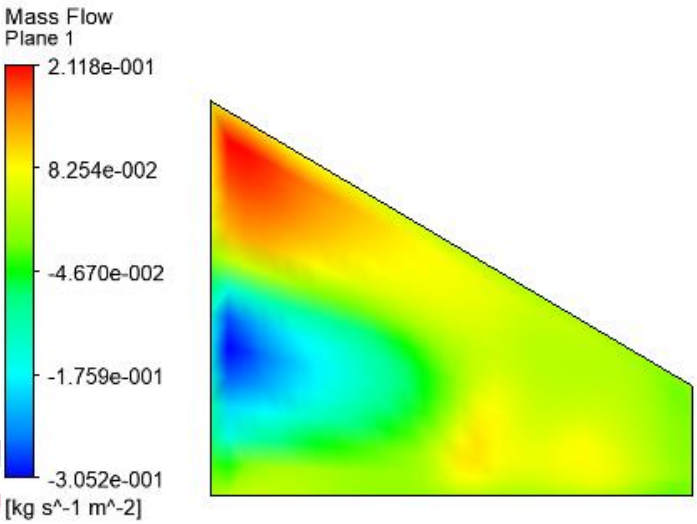

Fig. 10 Contour result of mass flow in the solar still for model 3

After performing computational fluid dynamics analysis on single slope solar still for mass flow of condense liquid following contour has been observed on a section in X-Y plane and at Z = 0.55 m, the maximum value of mass flow rate of 2.118e-1 kg/s-m^2 as shown in figure 4.7.

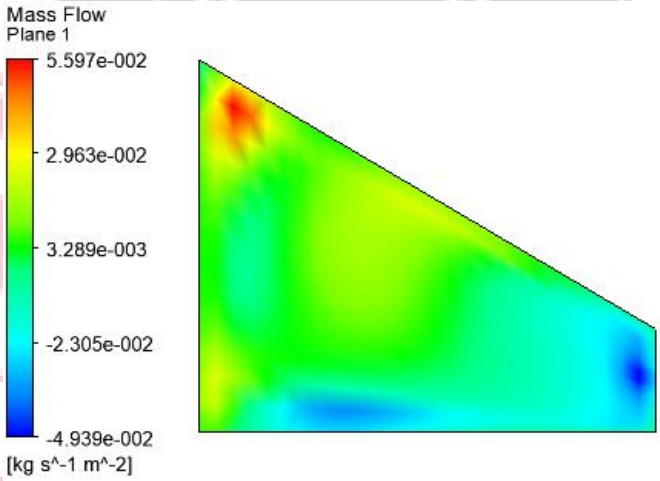

Fig. 11 Contour result of mass flow in the solar still for model 4

After performing computational fluid dynamics analysis on single slope solar still for mass flow of condense liquid following contour has been observed on a section in X-Y plane and at Z = 0.55 m, the maximum value of mass flow rate of 5.597e-2 kg/s-m^2 as shown in figure 4.8.

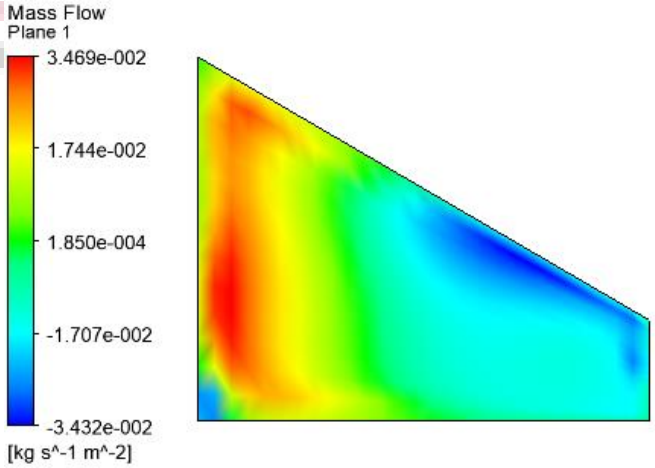

Fig. 12 Contour result of mass flow in the solar still for model 5

After performing computational fluid dynamics analysis on single slope solar still for mass flow of condense liquid following contour has been observed on a section in X-Y plane and at Z = 0.55 m, the maximum value of mass flow rate of 3.469e-2 kg/s-m^2 as shown in figure 4.9.

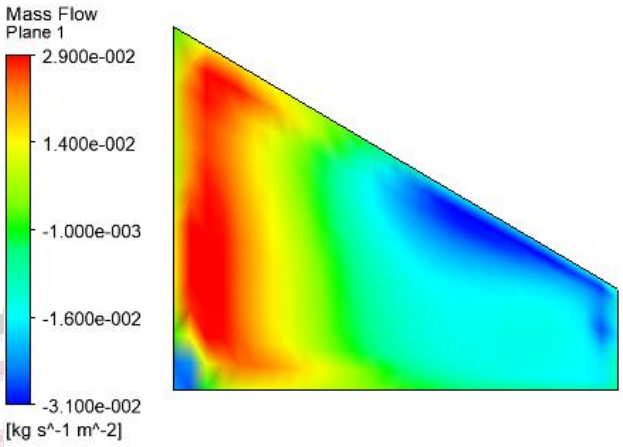

Fig. 13 Contour result of mass flow in the solar still for model 6

After performing computational fluid dynamics analysis on single slope solar still for mass flow of condense liquid following contour has been observed on a section in X-Y plane and at Z = 0.55 m, the maximum value of mass flow rate of 2.9e-2 kg/s-m^2 as shown in figure 4.10.

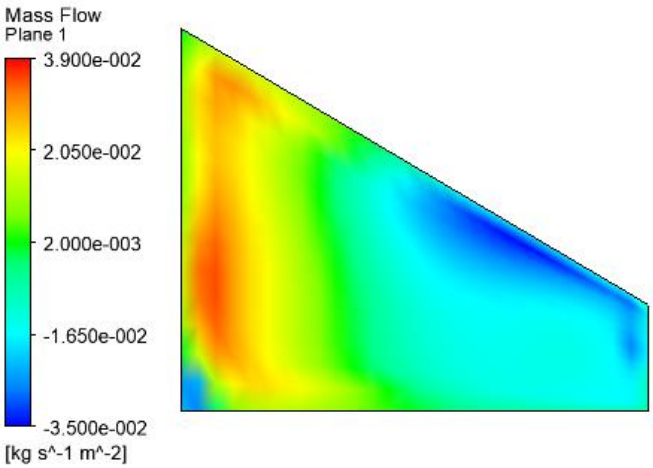

Fig. 14 Contour result of mass flow in the solar still for model 7

After performing computational fluid dynamics analysis on single slope solar still for mass flow of condense liquid following contour has been observed on a section in X-Y plane and at Z = 0.55 m, the maximum value of mass flow rate of 3.9e-2 kg/s-m^2 as shown in figure 4.11.

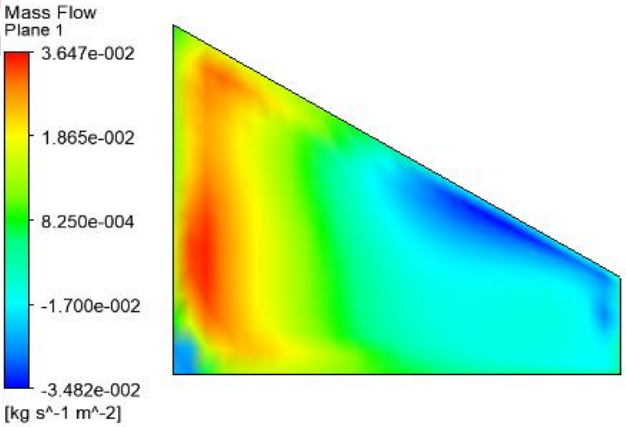

Fig. 15 Contour result of mass flow in the solar still for model 8

After performing computational fluid dynamics analysis on single slope solar still for mass flow of condense liquid following contour has been observed on a section in X-Y plane and at Z = 0.55 m, the maximum value of mass flow rate of 3.647e-2 kg/s-m^2 as shown in figure 4.12.

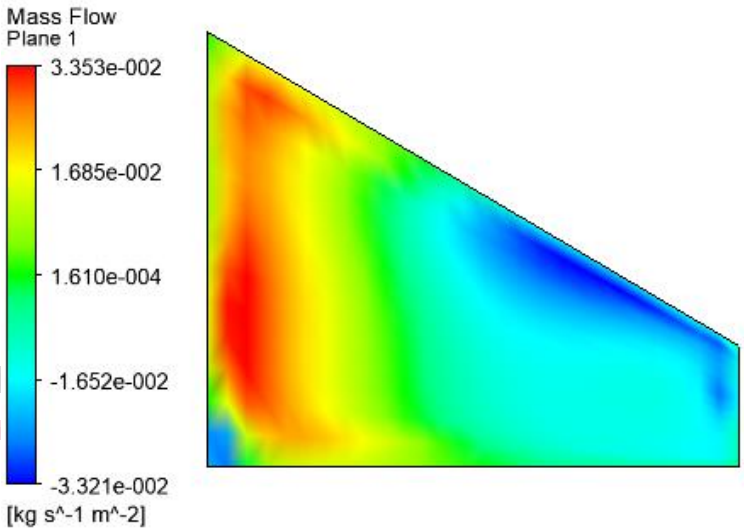

Fig. 16 Contour result of mass flow in the solar still for model 9

After performing computational fluid dynamics analysis on single slope solar still for mass flow of condense liquid following contour has been observed on a section in X-Y plane and at Z = 0.55 m, the maximum value of mass flow rate of 3.353e-2 kg/s-m^2 as shown in figure 4.13.

B. Simulation Results

Table 6 Simulation Results-L9 orthogonal array

Run	Slope	Glass thickness, m	Mass flow rate, Kg/s-m^2	Productivity, ml/hr
1	20º	0.01	0.0219	219.43
2	25º	0.02	0.0019	221.16
3	30º	0.03	0.2118	224.29
4	20º	0.02	0.0055	262.36
5	25º	0.03	0.0034	272.79
6	30º	0.02	0.029	291.22
7	20º	0.03	0.039	276.44
8	25º	0.01	0.0036	281.39
9	30º	0.02	0.0033	286.72

C. Optimisation

Table 4.3 shows the response table for vapour density.

Table 7 Response Table for Signal to Noise Ratios for mass flow

Level	Slope	Glass thickness, m
1	0.0785	0.0221
2	0.0126	0.0029
3	0.0153	0.0813
Delta	0.0659	0.0784
Rank	2	1

For each level of these factors, we have corresponding values of 0.0221, 0.0029, and 0.0813 for glass thickness; 0.0785, 0.0126, and 0.0153 for slope. The delta values represent the differences between the maximum and minimum values for each factor. In this case, the delta for slope is 0.0659, and the delta for glass thickness is 0.0784. The rank indicates the relative importance of each factor. In this case, for the factor "Slope," it has the smallest delta (0.0659), and thus, it has been assigned a rank of 2. For the factor "Glass thickness," it has a larger delta (0.0784), and it has been assigned a rank of 1.

Table 8 Response Table for Signal to Noise Ratios for productivity

Level	Slope	Glass thickness, m
1	46.91	48.01
2	48.79	48.20
3	48.99	48.48
Delta	2.08	0.47
Rank	1	2

For each level of these factors, we have corresponding values of 46.91, 48.79, and 48.99 for slope; 48.01, 48.2, and 48.48 for glass thickness. The delta values represent the differences between the maximum and minimum values for each factor. In this case, the delta for slope is 2.08, and the delta for glass thickness is 0.47. The rank indicates the relative importance of each factor. In this case, for the factor "Slope," it has the largest delta (2.08), and thus, it has been assigned a rank of 1. For the factor "Glass thickness," it has a smallest delta (0.47), and it has been assigned a rank of 2.

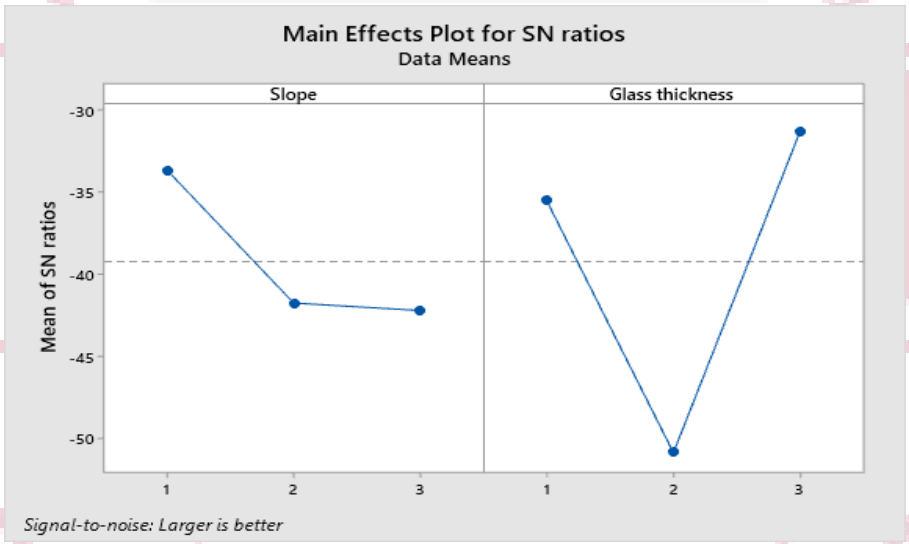

Fig. 17 Variation of slope and glass thickness on mass flow

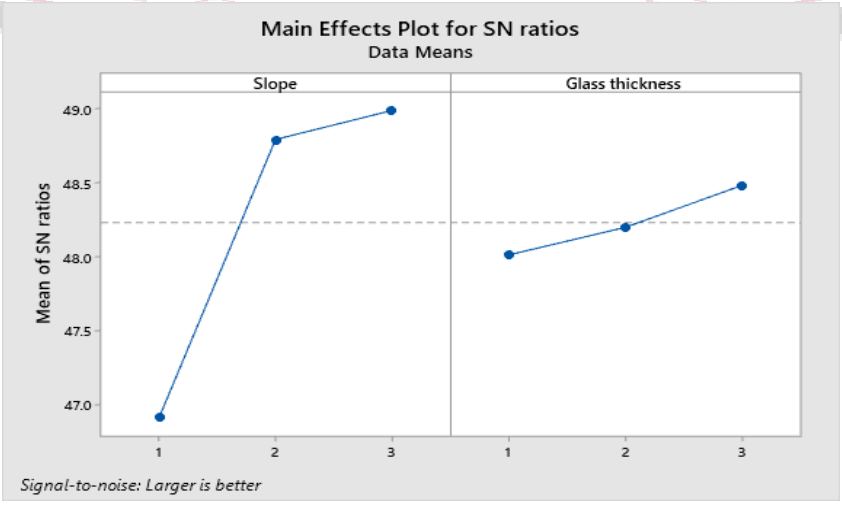

Fig. 18 Variation of slope and glass thickness on productivity

When the slope of a solar still increases, it can affect the collection and condensation of water vapor. A steeper slope might enhance the runoff of condensed water from the surface, leading to an initial increase in vapor density. This could be due to improved drainage, preventing the re-evaporation of condensed water. However, when the slope is doubled, it seems to have an adverse effect on vapor density. A very steep slope might cause water to flow too quickly, reducing the contact time between the condensing surface and the air. This reduced contact time can result in lower vapor density, as less water vapor has the opportunity to condense. Further based on fig. 4.15 and 4.15, the optimum parameter is A1B3 and A3B3.

D. Results Confirmation

Table 49 Parameter determination and comparison

Parameter	Conventional solar still	Optimized solar still
A1B3	0.0332	0.039 Kg/s-m^2
A3B3	221.67	224.24 ml/hr

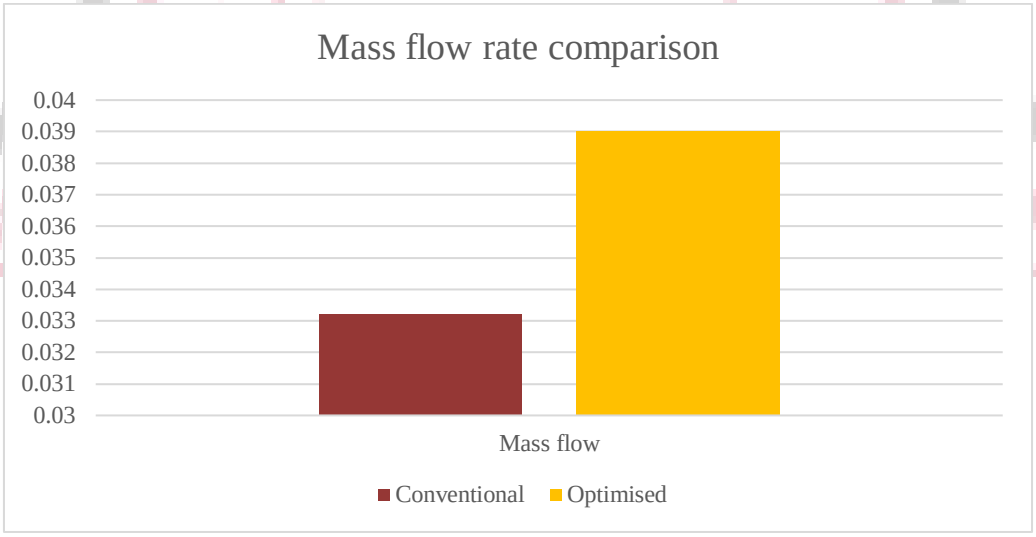

Fig. 19 Mass flow rate comparison

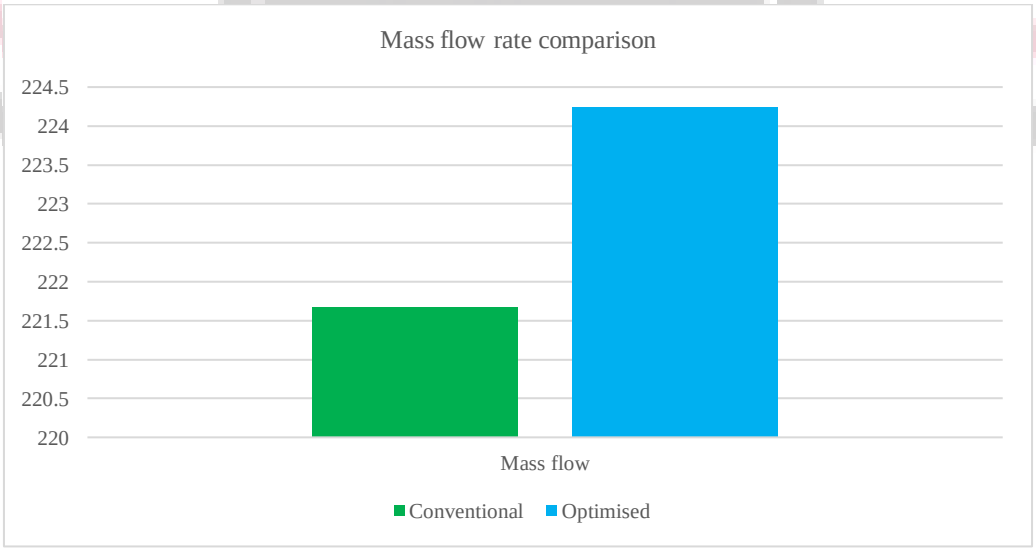

Fig. 20. Productivity comparison

Optimized results are compared with conventional model leads to improvement in mass flow rate from 0.0332 to 0.039 Kg/s-m^2 and improvement in productivity from 221.67 to 224.24 ml/hr.

VIII. CONCLUSION

This study demonstrates the effectiveness of employing computational fluid dynamics and the Taguchi method to optimize the performance of solar stills. By varying parameters such as glass thickness and slope angle, significant improvements in water productivity are achieved without compromising cost efficiency. The results indicate that careful selection of

design parameters is essential to maximize condensation efficiency and mass flow rate. The optimized solar still design, validated through CFD simulations, offers a promising solution for addressing water scarcity challenges in regions with abundant solar radiation. Further research could explore additional factors influencing solar still performance and validate the proposed optimization approach through experimental studies. Overall, this research contributes to advancing sustainable water production technologies, facilitating access to clean drinking water for communities worldwide.

REFERENCES

[1] Ojo, O. M., & Obiora-Okeke, O. A. (2022). Performance evaluation of a solar still for industrial wastewater treatment. Materials Today: Proceedings, 62, S1-S6.

[2] Shanmugan, S., Essa, F. A., Gorjian, S., Kabeel, A. E., Sathyamurthy, R., & Manokar, A. M. (2020). Experimental study on single slope single basin solar still using TiO2 nano layer for natural clean water invention. Journal of Energy Storage, 30, 101522.

[3] Arunkumar, T., Sathyamurthy, R., Denkenberger, D., & Lee, S. J. (2022). Solar distillation meets the real world: a review of solar stills purifying real wastewater and seawater. Environmental Science and Pollution Research, 29(16), 22860-22884.

[4] Afolabi, L. O., Enweremadu, C. C., Kareem, M. W., Arogundade, A. I., Irshad, K., Islam, S., ... & Didane, D. H. (2023). Experimental investigation of double slope solar still integrated with PCM nanoadditives microencapsulated thermal energy storage. Desalination, 553, 116477.

[5] Patel, S. K., Singh, D., Kumar, B., & Singh, D. (2020). Solar desalination technology: physicochemical parameters estimation of contaminated & treated water of gomti River, Lucknow (UP), India. Int. J. of Recent. Tech. and Engg, 8, 86-692.

[6] Roslan, J., Kan, W. E., Rahman, A. A., Suliman, M., & Isha, R. (2020). Charcoal characterization and application is solar evaporator for seawater desalination. In IOP Conference Series: Materials Science and Engineering (Vol. 736, No. 2, p. 022107). IOP Publishing.

[7] Kanka, S. D., Kibria, M. G., Anika, U. A., Das, B. K., Hossain, M. S., Roy, D., & Mohtasim, M. S. (2024). Impact of various environmental parameters and production enhancement techniques on direct solar still: A review. Solar Energy, 267, 112216.

[8] Sathyamurthy, R., Ali, H. M., Said, Z., El-Sebaey, M. S., Gopalsamy, S., Nagaraj, M., & Alomar, T. S. (2024). Enhancing solar still thermal performance: The role of surface coating and thermal energy storage in repurposed soda cans. Journal of Energy Storage, 77, 109807.

[9] da Silva Junior, L. G., de Oliveira, J. P. J., Ribeiro, G. B., & Ferreira Pinto, L. (2023). Experimental and Numerical Analysis of a Low-Cost Solar Still. Eng, 4(1), 380-403.

[10] Aghakhani, H., Ayatollahi, S. M., & Hajmohammadi, M. R. (2023). Proposing novel approaches for solar still performance enhancement by basin water heating, glass cooling, and vacuum creation. Desalination, 567, 117011.

[11] Hammoodi, K. A., Dhahad, H. A., Alawee, W. H., & Omara, Z. M. (2023). A detailed review of the factors impacting pyramid type solar still performance. Alexandria Engineering Journal, 66, 123-154.

[12] Shoeibi, S., Kargarsharifabad, H., Rahbar, N., Ahmadi, G., & Safaei, M. R. (2022). Performance evaluation of a solar still using hybrid nanofluid glass cooling-CFD simulation and environmental analysis. Sustainable Energy Technologies and Assessments, 49, 101728.

[13] S. El-Sebaey, M., Ellman, A., Hegazy, A., & Ghonim, T. (2020). Experimental analysis and CFD modeling for conventional basin-type solar still. Energies, 13(21), 5734.

[14] Nadgire, A. R., Barve, S. B., & Ithape, P. K. (2020). Experimental investigation and performance analysis of double-basin solar still using CFD techniques. Journal of the Institution of Engineers (India): Series C, 101, 531-539.

[15] Sonawane, C., Alrubaie, A. J., Panchal, H., Chamkha, A. J., Jaber, M. M., Oza, A. D., ... & Burduhos-Nergis, D. P. (2022). Investigation on the impact of different absorber materials in solar still using CFD simulation—economic and environmental analysis. Water, 14(19), 3031.